JMEPEG (2010) 19:1306–1310
DOI: 10.1007/s11665-010-9630-4

1059-9495/$19.00

Fracture of Open-Cell Nickel Foams Under Quasi-Static Tensile Loading

Mohamed Shehata Aly

(Submitted July 2, 2009; in revised form February 18, 2010)

Open-cell nickel foams with average pore size of 600 μm have been subjected to room temperature tensile tests to explore their tensile properties. Using a state of the art extensometer of noncontact type, foam properties as ultimate tensile strength, yield strength, and the Young's modulus (*E*) have been measured accurately. The reason behind the usage of this kind of extensometer is to avoid completely any minor deformation that might be caused by the attachment of conventional extensometer to the sample's surface prior to testing. The function of this extensometer is based on the usage of a laser (CCD) camera that detects and records the dimensional changes as soon as the load is applied. A series of cyclic loading-unloading tests was performed to determine the foam's Young's modulus. The fracture behavior of foam cells was observed to be ductile. Complete separation of struts or cell walls took place successively by necking.

Keywords mechanical properties, open-cell foams, powder metallurgy, tensile test

1. Introduction

Open and closed cell metal foams are becoming attractive for industrial applications as their manufacturing methods (Ref 1-6) develop quickly. Open-cell foams can be used as porous electrodes in rechargeable batteries (Ref 7, 8). There has been speculation that further benefit could be gained from the interconnectivity, open-cell structure and large surface-to-volume ratios of the foams (Ref 9-11).

Electrode structure is considered as a key factor in all rechargeable batteries. Their manufacturing starts with the production of a highly porous metal electrode made from nickel metal (Ref 10, 11). The nickel should exhibit porosity in excess of 95% (Ref 12), into which an active paste of electrochemical mass such as nickel oxide is infiltrated. The electrochemical performance of an electrode depends on the material from which it is made. As the charge, discharge, recharge, and overcharging processes result in volumetric changes of active mass, the electrode must have sufficient strength to avoid physical disintegration over time (Ref 9). Besides that, the electrode structure should exhibit a high degree of uniformity, be free from impurities and show a good density distribution (Ref 11). For smooth foam processing during the battery production, a high-tensile strength is necessary (Ref 12-14). For this reason, several research works (Ref 15-19) have recently been focused on exploring the tensile properties of porous metals. Liu (Ref 16) investigated the tensile behavior of open-cell nickel foam plates which were produced by electrodeposition on polyurethane sponge. Struts of this material were not fractured by necking; however, fracture takes place randomly following an avulsion mode. Using different theoretical relationships between biaxial nominal stresses and porosity, the tensile behavior for these materials was analyzed under biaxial stress tension (Ref 17, 18). Through combining the results of properties under uniaxial and biaxial tensions of these materials; a mathematical expression was gained for foamed metals under uniaxial and biaxial of collective tension and compression (Ref 19).

The objective of the present work is to explore the room temperature, quasi-static tensile behavior of powder metallurgy manufactured open-cell nickel foams.

Mohamed Shehata Aly, Center of Excellence for Research in Engineering Materials (CEREM), College of Engineering, King Saud University, 11421 Riyadh, Saudi Arabia and Central Metallurgical R&D Institute (CMRDI), P.O. Box 87, Helwan, Cairo, Egypt. Contact e-mail: drengshehata@yahoo.com.

2. Experimental Procedure

2.1 Sample Preparation

Open-cell nickel foams with porosities ≈96% (average pore size ≈ 600 μm) were supplied by Mitsubishi Materials Corporation in Japan. The foam samples were manufactured by a powder metallurgy technique, as illustrated schematically in Fig. 1. According to this process, nickel powder with a particle size of several hundred micrometers is mixed at room temperature with a foaming agent to form the foamy slurry. The slurry is cut into green samples which are left for drying. Afterward the green samples are sintered in a controlled atmosphere at a temperature of more than 1200 °C. The steps of the manufacturing process are explained in detail in Ref 20.

Figure 2 shows an optical image of a typical structure of the open-cell foams, taken at a magnification of 100 times by a digital microscope KEYENCE VHX-500. Open cells with struts connecting the cells are clearly visible. The pores are homogeneously distributed throughout the overall structure. The interconnected cell structure is obviously shown in Fig. 3. An average strut thickness of about 50 μm was measured.

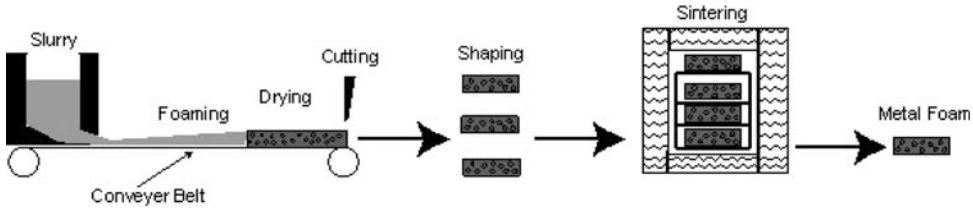

Fig. 1 A schematic drawing showing the main steps of the manufacturing process of open-cell nickel foams

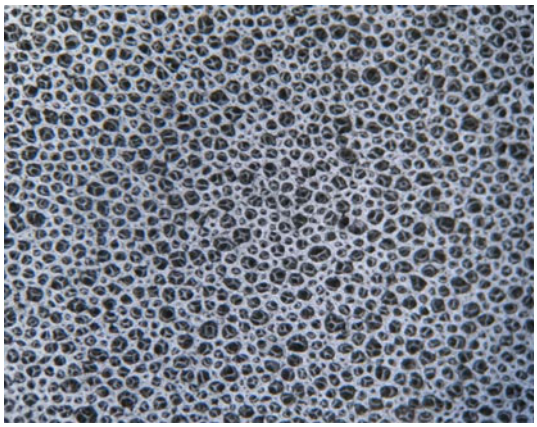

Fig. 2 Overall macroscopic structure of open-cell nickel foams

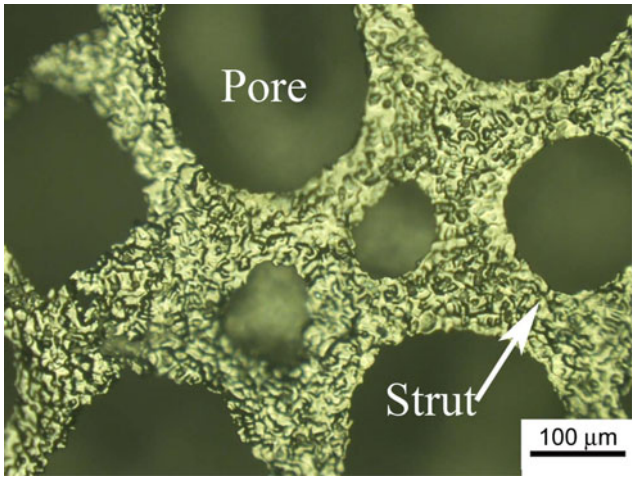

Fig. 3 The pore structure of open-cell nickel foams

The struts are considered to have a key role in the properties-structure relationship.

2.2 Tensile Test

To facilitate its gripping to the tensile testing machine, the tensile samples (10 mm wide × 100 mm long), were glued on both sides to aluminum tabs (with holes ∅5 mm) with an epoxy, as shown schematically in Fig. 4(a). Figure 4(b) shows the tensile foam sample clapped in the tensile machine during testing. The tensile tests were performed at room temperature under displacement control at a rate of 0.5 mm/min using a universal servo-hydraulic testing machine Autograph AG-50 kNG, Shimadzu. The machine is equipped with a load cell of 200 N. Unlike traditional extensometers which are attached to the sample's surface and may cause a deflection or deformation to the sample prior to loading, a noncontact-type extensometer was used to detect and record the resulting extension and thus any small deformation prior to testing will be avoided. The function of this extensometer is based on using a laser camera (DVW-200 Shimadzu). The camera records the extension occurs between two black markers clipped to the sample's surface, as shown in Fig. 4(b). The black markers define a gauge length of 50 mm. The experimental set-up (test machine, tensile sample, and the camera) is shown in Fig. 5.

The fracture mode was investigated by examining the struts' fracture surfaces using a scanning electron microscope (SEM) (Jeol, JSM-5410LS) equipped with an electron probe micro-analyzer (EPMA) (HITACHI S3500).

3. Results and Discussion

Figure 6 shows a typical tensile stress-strain curve of open-cell foam. The curve exhibits a nominally elastic strain, a yielding region followed by a hardening one and ends with fracture. The overall behavior is considered elasto-plastic. The elastic region initiates as the loading process starts and continues to small values of strain. As the applied load increases, the elastic zone stretches as well. A post-yielding, strain-hardening region increases gradually as the load increases. When the tensile force acts on the foamed body, the corresponding load concentrates on the end point of metallic struts, and this effect generates a bending moment on the metallic struts. This moment leads to a plastic deflection of the metallic struts to some extent due to the plastic hinge effect at the joint node of struts within the porous body (Ref 21). The struts rotate to become more aligned with the loading direction. Struts that are already aligned in this direction can only stretch and the amount of strain depends on the local topology (Ref 22). Based on the assumption that the bending moment is the main deformation mechanism of the foam, Duchamp et al. (Ref 23) presented a simple mechanical model for pure Ni in tension at room temperature. It incorporates the morphological parameters of foam volume fraction (Φ), the main axes of the cell (a, b, c) and the ratio of the equivalent axes ($R = b/a$ and $Q = c/a$) which represent the morphological anisotropy of the foam (Fig. 6). The idealized cell geometry of Fig. 6 is used to link the morphological parameters to the foam volume fraction (Φ):

$$\Phi = \frac{4t^2(a+b+c)}{abc} = \frac{4t^2}{a^2}\frac{Q+R+1}{RQ}, \qquad \text{(Eq 1)}$$

where t is the beams thickness. When the cell is deformed in the direction parallel to the RD, the beams parallel to TD and

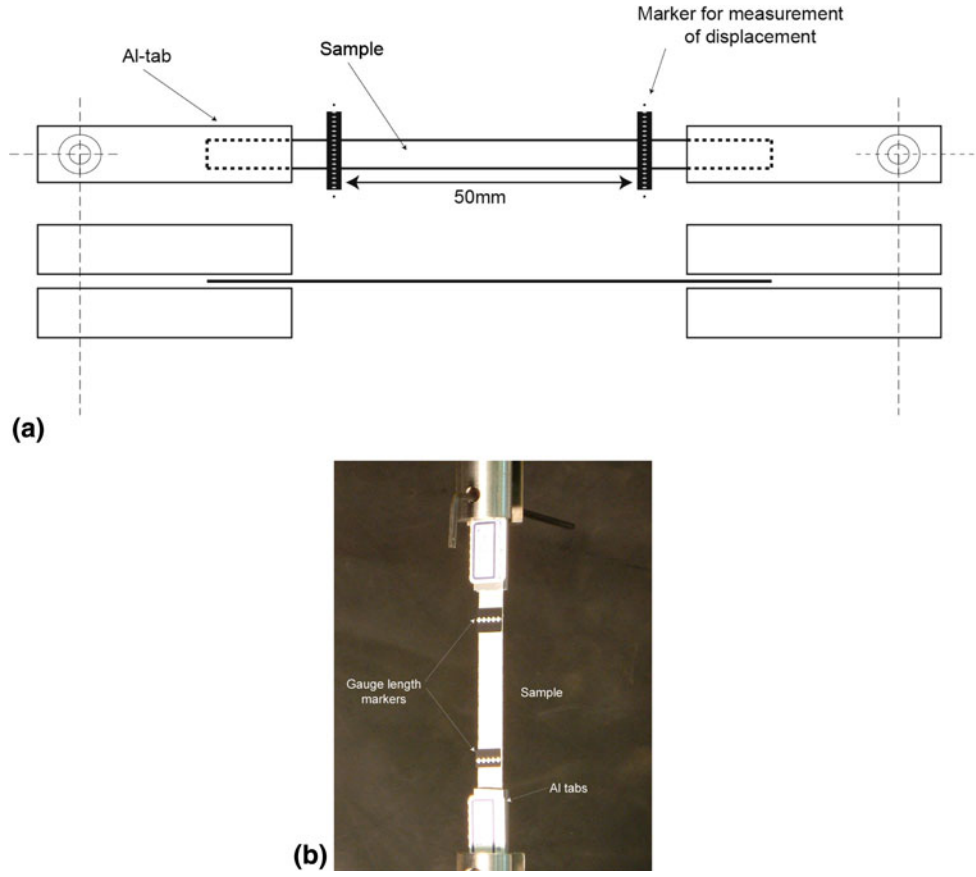

Fig. 4 (a) A schematic drawing shows the tensile sample with Al gripping tabs. (b) The tensile foam sample clapped in the tensile machine

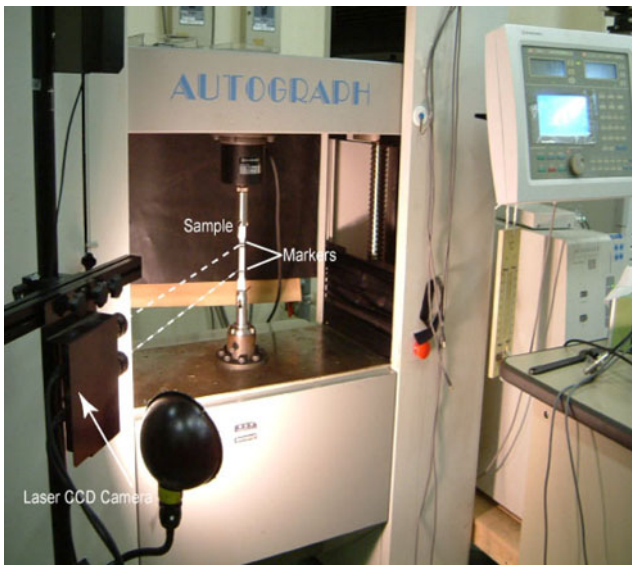

Fig. 5 Experimental set-up of the tensile test

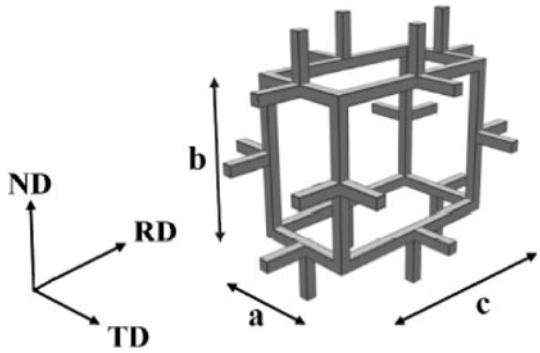

Fig. 6 A sketch of a simplified open-cell foam

ND are bent. When the foam is tested in the RD direction, then the beams of length *a* and *b* and of thickness *t* are bent.

If one of these struts contains a weak grain boundary and a highly realigning surrounding, this strut will fracture first (Ref 22), once the maximum stress at outer side of strut exceeds the failure strength of the corresponding solid metal. When a strut fails, stress redistribution occurs, causing the stress to reach the failure level for neighboring struts. A nonuniform strut thickness or strut containing voids weakens the foam mechanical properties (Ref 21).

As can be seen in Fig. 7 and 8, failure of foam samples under tensile loading proceeds with the consecutive failure of struts, following a zigzag-like path forming a fracture plane that is more or less perpendicular to the loading direction.

From the curve depicted in Fig. 7, it can be seen that the foam sample yielded at a stress of about 0.3 MPa. The ultimate strain was found to be 5.5% at a fracture stress of about 0.65 MPa. Table 1 gives the mechanical properties of three foam samples. The measured values gave an indication that the

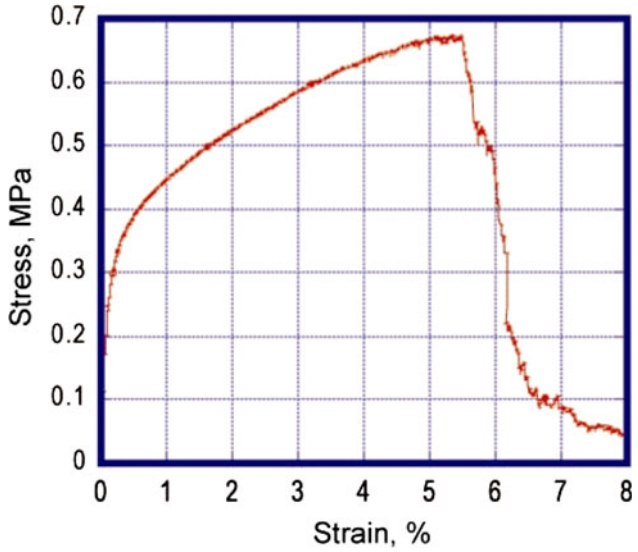

Fig. 7 Tensile stress-strain curve of open-cell nickel foam

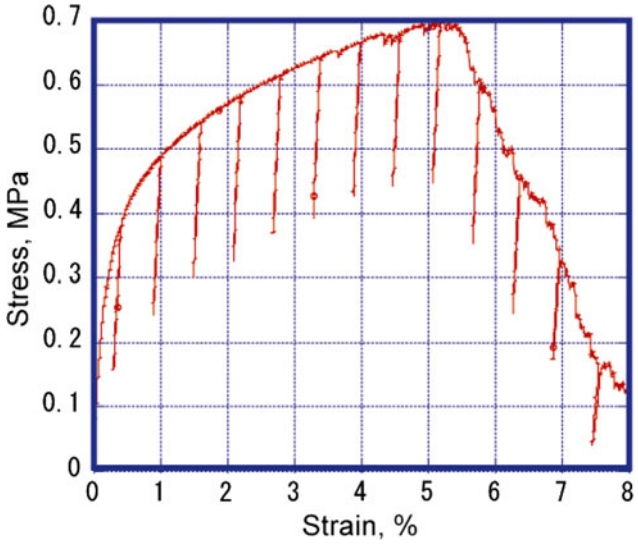

Fig. 8 Cyclic loading-unloading tensile stress-strain curve of open-cell nickel foam

Table 1 Mechanical properties of different samples of Ni foams

Sample	YS, MPa	UTS, MPa	ε, %
1	0.32	0.70	5.4
2	0.30	0.65	5.6
3	0.35	0.74	4.6

foam structure of all samples was homogeneous. Due to the yielding of some cells at small loads, repeated loading-unloading tests, as shown in Fig. 8, were carried out to measure the Young's modulus which is a measure of foam's stiffness. An average value of about 0.25 GPa was measured. The minor changes in the measured Young's modulus values at different strains are probably due to the variation in the microstructure, pore size, and pore distribution throughout the

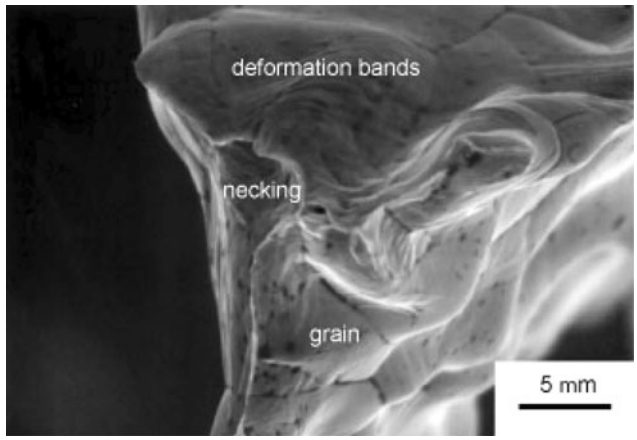

Fig. 9 SEM micrograph of a fractured strut of nickel foam sample

struts and this may interpret the small differences in the stress-strain behaviors shown in Fig. 7 and 8, respectively.

A SEM micrograph, as shown in Fig. 9, reveals that the fracture of strut took place transgranularly and substantial necking was observed. In addition, deformation slip bands were clearly visible. This mode of fracture varies with the processing technique. For example, fracture of open-cell nickel foams produced by electro-deposition technique takes place trans-granular, since the presence of ductility deteriorating elements like sulfur makes grain boundaries very brittle (Ref 13).

Nonhomogeneous distributed, dark tiny nanopores were observed throughout the strut. This may lead to a decrease in the foam's strength since they hinder the movement of dislocations (Ref 13). On the other side, grain growth will be interrupted when the structure is enriched with nanopores (Ref 12).

4. Conclusions

In this study tensile tests were performed on open-cell nickel foams with average pore size of 600 μm. By means of a laser CCD camera which acts as a noncontact-type extensometer, the tensile properties were measured accurately. A typical stress-strain curve with its three distinguishable regions was obtained. Fracture of struts, which is of ductile mode, took place by necking and proceeded successively starting from the weakest strut.

Acknowledgments

The author thank the Japanese Society for the Promotion of Science (JSPS) for the financial support. The fruitful discussion with Prof. Shojiro Ochiai from Kyoto University is highly appreciated. The author is greatly thankful to Mr. K. Kita, K. Kato, and K. Honma from Mitsubishi Materials Corporation in Japan for providing the foamed samples.

References

1. O.B. Olurin, K.Y.G. McCullough, N.A. Fleck, and M.F. Ashby, Fatigue Crack Propagation in Aluminum Alloy Foams, *Int. J. Fatigue*, 2001, **23**, p 375–382
2. J. Baumeister and J. Schrader, "Methods for Manufacturing Foamable Metal Bodies," German Patent DE 41 01 630, 1991

3. G.J. Davies and S. Zhen, Metallic Foams: Their Production Properties and Applications, *J. Mater. Sci.*, 1983, **18**, p 1899–1911
4. S. Akiyama, K. Imagawa, A. Kitahara, S. Nagata, K. Morimoto, T. Nishikawa, et al. "Foamed Metal and Method of Producing the Same." US Patent 4,713,277, 1987
5. H. Sang, "Process for Producing Shaped Slabs of Particle Stabilized Foamed Metal." US Patent 5,334,236, 1994
6. J. Banhart, Ed., *Proceedings of Metallschaum Conference on Metal Foams*, MIT Publications, Bremen, Germany, 1997
7. P.S. Liu, T.F. Li, and C. Fu, Relationship Between Electrical Resistivity and Porosity for Porous Metals, *Mater. Sci. Eng.*, 1999, **A268**, p 208–215
8. J. Banhart, Manufacture, Characterization and Application of Cellular Metals and Metal Foams, *Prog. Mater. Sci.*, 2001, **46**, p 559–632
9. L.J. Gibson and M.F. Ashby, *Cellular Solids-Structure and Properties*, 2nd ed., Cambridge University Press, Cambridge, UK, 1997
10. V.A. Ettel, New Inco Powder and Foams for Nickel Batteries. In: *NiCd' 98 8th International Nickel-Cadmium Battery Conference*, Prague, Sept. 21-22, 1998, p 197–200
11. O.B. Olurin, S.W. David, C.W. George, V. Paserin, and J. Shu, Strength and Ductility of As-Plated and Sintered CVD Nickel Foams, *Comp. Sci. Tech.*, 2003, **63**, p 2317–2329
12. G.J.C. Carpenter, Z.S. Wronski, and M.W. Phaneuf, TEM Study of Nanopores and the Embrittlement of CVD Nickel Foam, *Mater. Sci. Tech.*, 2004, **20**, p 1421–1426
13. V. Paserin, J. Shu, and S. Marcuson, Superior Nickel Foam Production: Starting from Raw Materials Quality Control, *Porous Metals and Metal Foaming Technology*, H. Nakajima and N Kanetake, Ed., The Japan Institute of Metals, 2005
14. X. Badiche, S. Forest, T. Guibert, Y. Bienvenu, J.D. Brtout, P. Ienny, M. Croset, and H. Bernet, Mechanical Properties and Non-Homogeneous Deformation of Open-Cell Nickel Foams: Application of the Mechanics of Cellular Solids and Porous Materials, *Mater. Sci. Eng.*, 2000, **289**, p 276–288
15. P.S. Liu, Tensile Strength of Porous Metals with High Porosity, *J. Adv. Mater.*, 2000, **32**, p 9–16
16. P.S. Liu, Tensile Fracture Behavior of Foamed Metallic Materials, *Mater. Sci. Eng.*, 2004, **A384**, p 352–354
17. P.S. Liu, Mechanical Behaviors of Porous Metals Under Biaxial Tensile Loads, *Mater. Sci. Eng.*, 2006, **A422**, p 176–183
18. P.S. Liu, A New Analytical Model About the Relationship Between Nominal Failure Stresses and Porosity for Foamed Metals Under Biaxial Tension, *Mater. Des.*, 2007, **28**, p 2678–2683
19. P.S. Liu and G.F. Chen, Mechanical Relation of Foamed Metals Under Uniaxial and Biaxial Loads of Collective Tension and Compression, *Mater. Sci. Eng.*, 2009, **A507**, p 190–193
20. W. Masahiro, *Processing of Metal Foams Using Slurry Technique*, Chemical Society of Japan 54, 2001, p 7–9
21. M. Shehata Aly, A. Almajid, S. Nakano, and S. Ochiai, Fracture of Open Cell Copper Foams Under Tension, *Mater. Sci. Eng.*, 2009, **A519**, p 211–213
22. E. Amsterdam, P.R. Onck, J. Th, and M. De Hosson, Fracture and Microstructure of Open Cell Aluminum Foam, *J. Mater. Sci.*, 2005, **40**, p 5813–5819
23. M. Duchamp, J.D. Bartout, S. Forest, Y. Bienvenu, G. Walther, S. Saberi, and A. Boehm, *Mechanical Behavior of Nickel Base Foams for Diesel Particle Filter applications*, Mechanical Properties of Cellular Materials, France, 2007